

# Influence of orientation angles on field emission characteristics of boron nanotubes: a theoretical study

SHUNFU XU<sup>a,b</sup>, WEIHUI LIU<sup>c</sup>, GUANG YUAN<sup>d</sup>

<sup>a</sup>*Institute of Architecture and Engineering, Weifang University of Science and Technology Weifang 262700, China*

<sup>b</sup>*Institute of Architecture and Engineering, Shandong Vocational College of Science and Technology Weifang 261053, China*

<sup>c</sup>*Department of Physics, Shandong University of Science and Technology, Qingdao 266590, China*

<sup>d</sup>*Department of Physics, Institute of Information Science and Engineering, Ocean University of China, Qingdao 266100, China*

The field emission characteristics of tilted nanomaterials depend notably on their inclination angles. Therefore, in this paper, the significant influence of orientation angles (OAs for short) on field emission characteristics of a capped (5, 5) boron nanotube (BNT) was investigated using density functional theory calculations. Their work functions with different OAs decreased linearly with applied electric fields, and emission currents increased distinctly with external electric fields. There was a small difference among these work functions under lower electric fields. However, distinctions of work functions and emission currents were enlarged while the external fields ranged from  $-0.1 \text{ V/\AA}$  to higher value. The emission currents of the (5, 5) BNT under applied electric fields were comparable to that of carbon nanotubes (CNTs) under the same electric fields, and the apex of the (5, 5) BNT were the highest probable positions for electron emission. The tunneling probability of the pristine (5, 5) BNT with  $OA=0$  reached maximum value, so that the BNTs perpendicular to the substrate would achieve the largest emission current.

(Received June 6, 2016; accepted November 28, 2017)

*Keywords:* Boron nanotube, Orientation angle, Field emission, Work function, Emission current, Tunneling probability.

## 1. Introduction

Nanomaterials such as carbon nanotubes, graphene and monolayer transitional metal chalcogenides are potential structures to meet the demands of future nanotechnology. In recent decades, carbon nanotubes [1] have attracted diverse interests as promising raw material for new nano-electronics because of their special electronic property and geometry. The applications of carbon nanotubes in field emission devices have been fully demonstrated in particular [2-3]. Boron, as carbon, also has attracted wide attention due to its advantages as candidates of superhard material [4-6]. In recent years, several new boron structures have been presented [7-12]. Thereinto, the pure boron nanotubes have been prepared in 2004 [13-15]. Similarly, boron nanotubes are constructed by curling up two dimensional nanosheets along a certain direction. In contrast to carbon nanotubes, all boron nanotubes are predicted to be metallic and have large densities of states at their Fermi energies, regardless of diameter or chirality [16]. Therefore, the BNTs should be better metallic systems for one-dimensional electronics and may have higher superconducting temperature than

CNTs.

Liu et al. [14] found that individual boron nanotubes can achieve a high current of  $80 \times 10^{-5} \text{ A}$  and a current density of  $2.04 \times 10^{11} \text{ A/m}^2$ . The experimental work function is 4.52 eV, which may be lower than that of CNTs ( $\sim 4.80 \text{ eV}$ ) [17]. Considering the BNTs fabricated by Liu et al. [13] possessing good field emission properties, [14] they should be useful for particular applications in field emitters, light emitting diodes, organic light-emitting diode, etc. The calculated work function of boron  $\alpha$ -sheet (4.11 eV) [13] is in accord with the experimental value [14]. Therefore, the actual structure of boron nanotubes may stem from the  $\alpha$ -sheet.

The work functions and field emission characteristics were engineered using an external electric field, [18] chemical and metal dopings, [19] substrate orientations, [20] and self-assembled monolayers or metal oxide layers [21] for the design of nanoscale electric devices. Thus, modulation for the work functions and field emission characteristics of boron nanotubes on atomic scale is crucial for maximizing device performance. Recently, the orientation of aligned CNTs has gotten attention and it has been shown that it is possible to grow CNTs with an

orientation angle different from the vertical in local areas [22–25]. Experimental results show that the field emission characteristics (particularly the electrical field enhancement factor) of a tilted nanotube depend notably on the inclination angle [26]. However, so far there is no report in field emission characteristics of capped BNTs with different orientation angles.

In this letter, we present the influence of OA on field emission characteristics of BNTs (here we selected a typical BNT which derived from  $\alpha$ -sheet [27] single-walled armchair (5, 5) BNT) using density functional theory calculations. The simulation results reveal that the boron atoms at the apex (emission surface) of the BNT are the highest probable positions for electron

emission.

## 2. Calculation details

Fig. 1 displays the atomic structure of the armchair (5, 5)  $\alpha$ -BNT which originates from the boron  $\alpha$ -sheet. The (5, 5) BNT consists of a six-layer stem along tube axis, a hemisphere of  $B_{80}$  fullerene, and ten hydrogen atoms. The orientation (inclination) angles were modeled by rotating tube axis (Z axis) of the (5, 5) BNT in YOZ plane with different angles:  $N*\pi/12$  ( $N=0, 1, 2, 3, 4, 5, 6$  and  $7$ ), which are illustrated in Fig. 1(a).

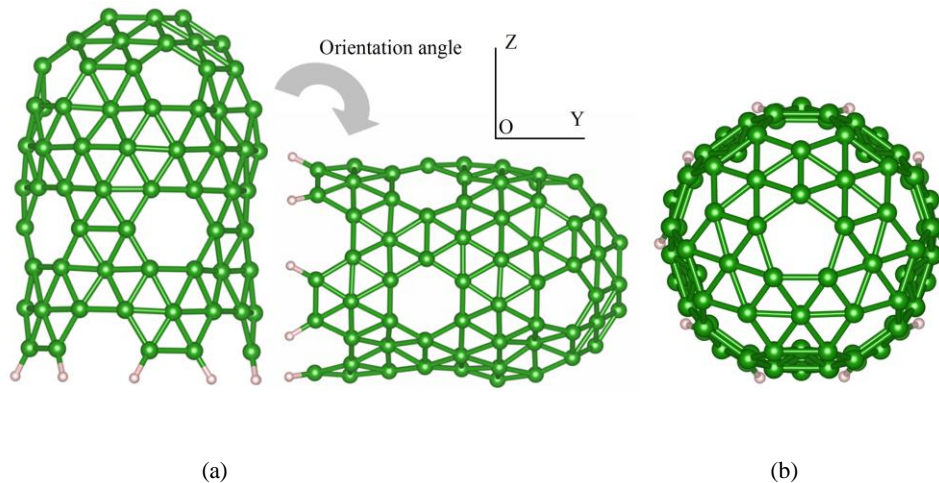


Fig. 1. (Color Online) Side view of (a) (5, 5) boron nanotube (orientation angles were modeled by rotating tube axis of the (5, 5) BNT in YOZ plane with different angles ( $OA=0, \pi/12, \pi/6, \pi/4, \pi/3, 5\pi/12, \pi/2$ ) and top view of (b) (5, 5) boron nanotube with a hemisphere of  $B_{80}$  at one end. Green and purple balls represent B and H atoms, respectively.

Our research was carried out using density functional theory (DFT) under Perdew–Burke–Ernzerhof (PBE) generalized gradient approximation (GGA) [28]. A tetragonal supercell was constructed with a vacuum width of 3.0/3.5 nm along X/Z axis to avoid corresponding deviations. The  $\Gamma$  point approximation was used to sample the Brillouin zone. The structure was fully optimized with an energy cutoff of 400 eV. We had exerted dipole and potential correction [29–30] on structure optimization. We had also taken into account the van der Waals (vdW) interactions by using DFT-D2 functional within GGA-PBE [31–32].

The work function was defined as  $W_F = V_l - E_f$  ( $V_l$  represents vacuum level and  $E_f$  denotes Fermi level) [33]. All structure optimization was carried out using the pwscf package, a suite of codes for ab initio electronic-structure calculations [34–35]. The emission currents under external fields were achieved using theory from Khazaei et al. [36]. The supercell was separated by a fine mesh ( $80 \times 192 \times 192$ ), and the emission current was obtained by integrating all the currents from all elements of the mesh.

## 3. Calculation results and discussion

The work function of the pristine capped (5, 5) BNT (with  $OA=0$ ) along Z-axis/X-axis ( $WF_Z/W_FX$ ) is 4.69/4.72 eV, which is higher than that of our calculation results of pristine capped (5, 5) CNTs (4.20 eV) in Ref. 37. The higher work functions than that presented in Liu et al. [14] are based on participation of the  $B_{80}$  hemisphere.

To research the field emission characteristics of the (5, 5) BNT, a uniform electric field ( $E=-0.1, -0.2, -0.3, -0.4$  and  $-0.5$  V/Å, which are approximately equal to the electric field in experiments [14]), is applied along tube axis (Z axis). The structural change after relaxation is rather small under applied fields. Fig. 2 shows the work functions of the (5, 5) BNT along Z-axis with different orientation angles plotted against the applied electric fields (The work functions shown in Fig. 2 only have relative significance in investigating the difficulty level of emitting electrons and influence of electric fields on them. The real definition of work function in solid state physics is the

work function under  $0 \text{ V/\AA}$ ). As shown in Fig. 2, the work functions of the (5, 5) BNT decrease linearly with applied electric fields. The linear dependence on electric fields indicates that the work functions of the (5, 5) BNT can be simply manipulated by applied electric fields.

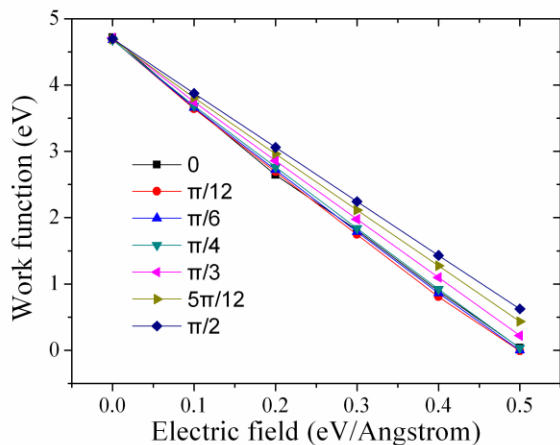


Fig. 2. (Color Online) Work functions of the (5, 5) BNT with different orientation angles versus electric fields

There was a small difference among work functions under  $0 \text{ V/\AA}$  for the (5, 5) BNT with different orientation angles. However, the difference was enlarged while the external fields changed from  $0 \text{ V/\AA}$  to  $-0.5 \text{ V/\AA}$ . Moreover, the work functions decrease evidently with the OAs. The (5, 5) BNT with  $OA=0$  possesses the lowest work functions under all electric fields. Our result shows that the fluctuation of  $W_F$  is mostly due to the change of vacuum levels, while the shift of Fermi levels has only a very slight impact. To be precise, the Fermi/vacuum level shift of the (5, 5) BNT under  $-0.5 \text{ V/\AA}$  is  $+0.54/-4.30 \text{ eV}$ , and variation of work function is  $-3.74 \text{ eV}$ . Moreover, other types of BNTs such as (9, 0) and (5, 0) BNTs are presumed to have similar phenomenon as the (5, 5) BNT.

Due to the influence of applied electric fields, the electrons are easily transferred from bottom to top of the BNTs. Fig. 3 shows the differential charge density (DCD for short) of the (5, 5) BNT with different orientation angles ( $OA=0, \pi/4$  and  $\pi/2$ ) under  $-0.5 \text{ V/\AA}$ . The DCD accumulate on apexes after applying the electric fields, exhibiting features of a  $\pi$  molecular orbit (especially for  $OA=0$ ) on the apices. The redistribution of electric charge will elevate the Fermi levels and decrease the vacuum levels. The DCD of the (5, 5) BNT with other orientation angles is similar to the previously discussed DCD. Furthermore, the DCD under stronger electric fields are presumed to be more evident in charge transfer and Fermi/vacuum level shift.

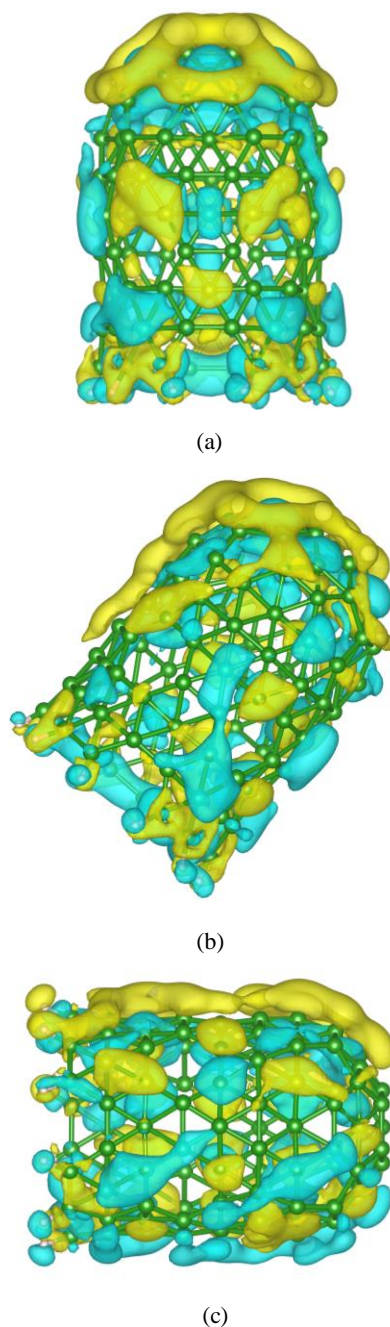


Fig. 3. (Color Online) 3D contours for differential charge density distributions of the (5, 5) BNT with (a)  $OA=0$ , (b)  $OA=\pi/4$  and (c)  $OA=\pi/2$  under  $-0.5 \text{ V/\AA}$ .

Fig. 4 illustrates the density of states (DOS for short) of the (5, 5) BNT under  $-0.1, -0.2, -0.3, -0.4$  and  $-0.5 \text{ V/\AA}$  with  $OA=0$ , and Fig. 5 gives the DOS of the (5, 5) BNT with different orientation angles ( $OA=0, \pi/4$  and  $\pi/2$ ) under  $-0.5 \text{ V/\AA}$ . As shown in Fig. 4, the capped (5, 5) BNT presents semiconducting properties because of presence of hemisphere of  $B_{80}$ . The density of states of the (5, 5) BNT under different electric fields have no distinct difference except for the Fermi levels. From Fig. 5, it is evident that the DOS of the (5, 5) BNT with different orientation angles have also no distinct change except for the Fermi

levels.

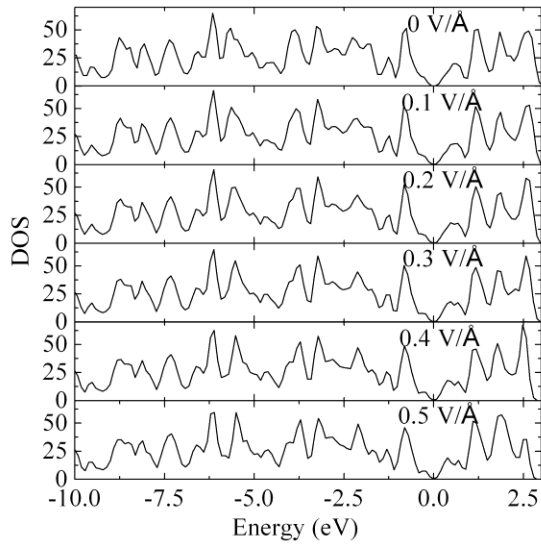


Fig. 4. Density of states (DOS) of the (5, 5) BNT with  $OA = 0$  under different electric fields (0~ $-0.5$  V/Å). Fermi levels are set to 0 eV.

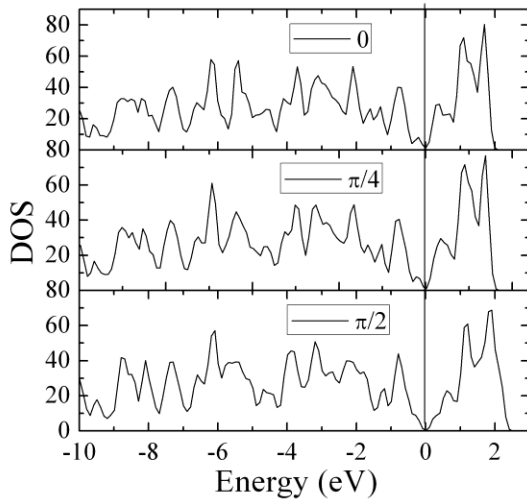


Fig. 5. Density of states (DOS) of the (5, 5) BNT with different orientation angles ( $OA = 0, \pi/4$  and  $\pi/2$ ) under  $-0.5$  V/Å. Fermi levels are set to 0 eV.

Fig. 6 shows the projected density of states (PDOS for short) of a boron atom on apex (emission surface) of the (5, 5) BNT with different orientation angles ( $OA = 0, \pi/4$  and  $\pi/2$ ) under 0 and  $-0.5$  V/Å. For the (5, 5) BNT under 0 V/Å, the PDOS of boron atoms near the  $E_f$  is mostly due to  $2p_z$  orbitals of boron atoms. After applying an electric field ( $-0.5$  V/Å), the PDOS of boron atoms with  $OA = 0$  and  $\pi/4$  has also no distinct change except for the Fermi levels. However, the PDOS near the  $E_f$  is mostly due to  $2p_x$  and  $2p_y$  orbitals of the boron atoms while the orientation angle change from 0 to  $\pi/2$ , which reveals charge transfer from  $2p_z$  orbit to  $2p_x$  and  $2p_y$  orbitals of boron atoms on the apex.

These characteristics are consistent with differential charge density distribution as shown in Fig. 3. Furthermore, charge transfer from  $2p_z$  orbital to  $2p_x + 2p_y$  orbitals of boron atoms depresses the Fermi levels and enhances the work functions. Similar properties of PDOS are found for the (5, 5) BNT with other orientation angles and electric fields.

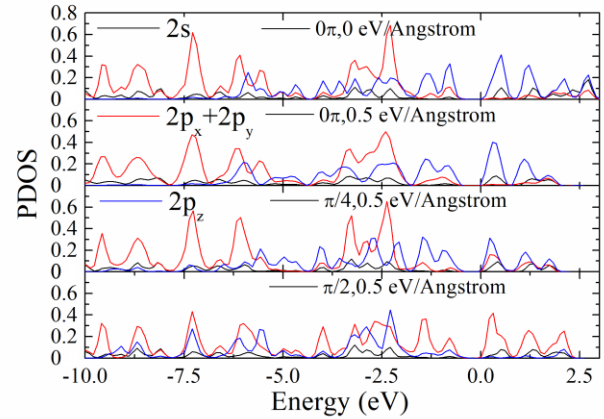
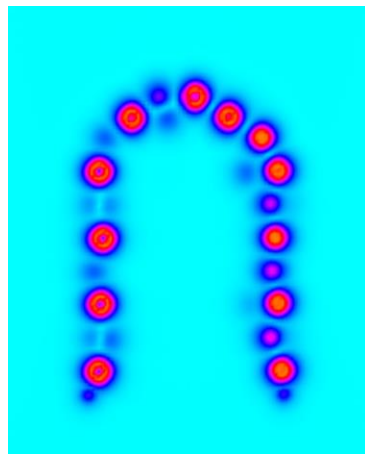


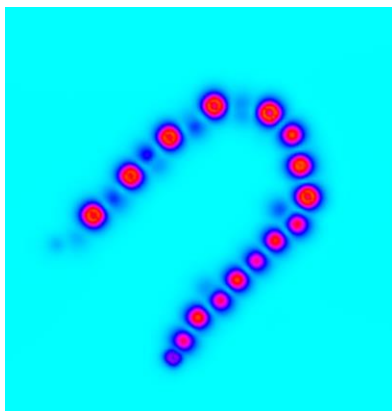
Fig. 6. (Color Online) PDOS of boron atoms in the first layer of the (5, 5) BNT with different orientation angles ( $OA = 0, \pi/4$  and  $\pi/2$ ) under  $-0.5$  V/Å.

The field emission properties depend on many other factors including field enhancement factor, tunneling probability, electronic occupation of orbit, and electron density on emission site. Fig. 7 illustrates the 2D contours for electric field distribution of the (5, 5) BNT with different orientation angles ( $OA = 0, \pi/4$  and  $\pi/2$ ) under  $-0.5$  V/Å. From this figure, we can clearly observe that the boron atoms on apex of the (5, 5) BNT plays an important role in electron emission because of the strongest electric field. However, the orientation angles have almost no influence on field enhancement factor of the (5, 5) BNT (2220/2220/2217 for  $OA = 0, \pi/4$  and  $\pi/2$  in our calculation).

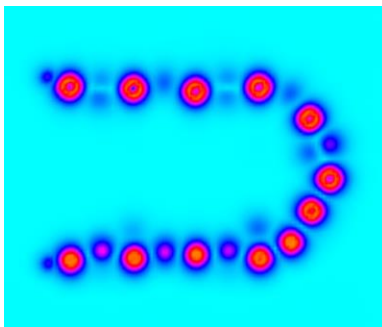
Fig. 8(a)-(c) displays the patterns of tunneling probability (TP for short) of the pristine (5, 5) BNTs with different orientation angles ( $OA = 0, \pi/4$  and  $\pi/2$ ) under  $-0.5$  V/Å, wherein the bright spots correspond to sharp area of apex of the (5, 5) BNT. Saito et al. [38] and Kuzumaki et al. [39] concluded from a field emission microscopy image of a carbon nanotip that most probable emission sites located either on center pentagon or on neighboring atoms. However, our first-principles results show that, under the influence of orientation angle, the most probable emission sites are not necessarily the center pentagons/hexagons. And the boron atoms on the tip of the pristine (5, 5) BNTs and their adjacent bonds are the highest probable positions for electron emission under an external field.



(a)

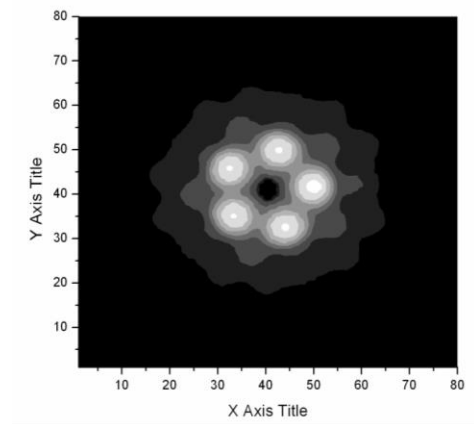


(b)

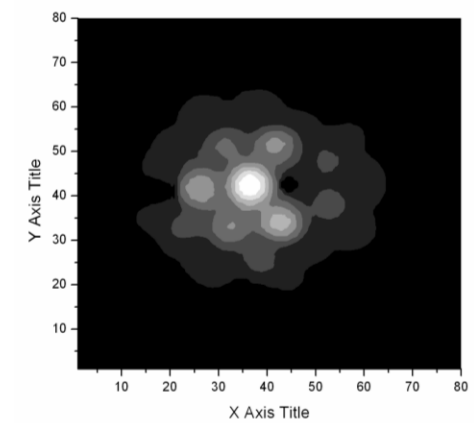


(c)

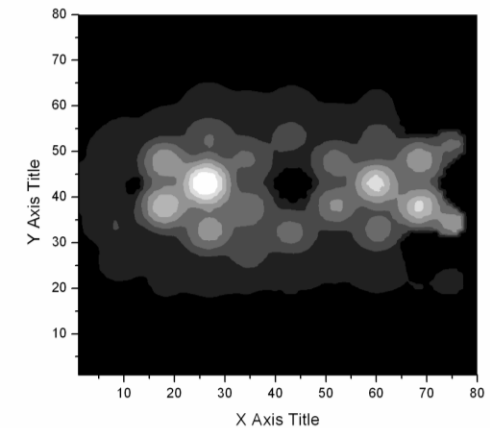
Fig. 7. (Color Online) 2D Contour for electric field distribution of the (5, 5) BNT with different orientation angles ((a)  $OA=0$ , (b)  $OA=\pi/4$ , (c)  $OA=\pi/2$ ) under  $-0.5$  V/Å. Color depth denotes different values of electric field intensity.



(a)



(b)



(c)

Fig. 8. Total tunneling probability pattern for (a) the (5, 5) BNT under  $-0.5$  V/Å with  $OA=0$ , (b) the (5, 5) BNT under  $-0.5$  V/Å with  $OA=\pi/4$ , (c) the (5, 5) BNT under  $-0.5$  V/Å with  $OA=\pi/2$ . Luminance in the pattern denotes different values of the tunneling probability.

We have also achieved localized electron density (LED for short) of the (5, 5) BNT under applied electric fields with different orientation angles ( $OA=0, \pi/4$  and  $\pi/2$ ), and Fig. 9 shows the LED for molecule orbits associated with the largest emission currents. As shown in Fig. 9(a)-(b), the localized electron density is mainly localized around pentagon and hexagon rings on the emission surface (apex) of the (5, 5) BNT. Therefore, the pentagons/hexagons on apex own both maximum TP and

maximum LED, and then the molecule orbital achieves the largest current on pentagon/hexagon. In addition, energy orbits localized on the other pentagons/hexagons and sidewall result in smaller emission currents than that of the degenerated energy orbits mentioned above. As shown in Fig. 9(c), the localized electron density is mainly localized on sidewall. Consequently, the degenerated energy orbital approximately contributes largest emission current on sidewall.

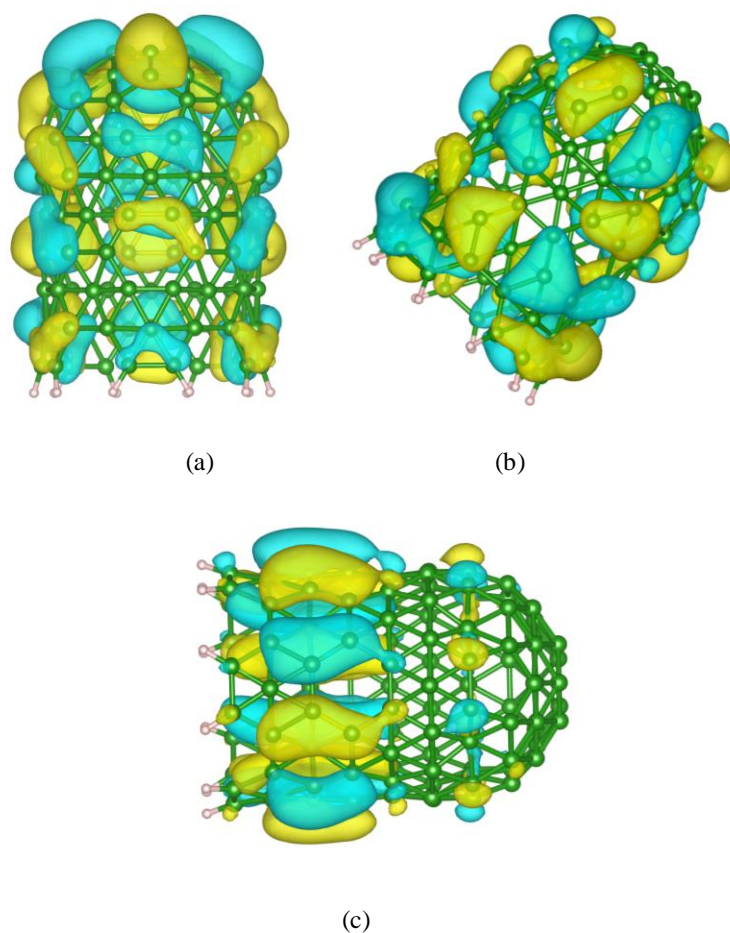


Fig. 9. (Color Online) The electron density of orbits which have the largest emission currents for (a) the (5, 5) BNT under  $-0.5 \text{ V/\AA}$  with  $OA=0$ , (b) the (5, 5) BNT under  $-0.5 \text{ V/\AA}$  with  $OA= \pi/4$ , (c) the (5, 5) BNT under  $-0.5 \text{ V/\AA}$  with  $OA= \pi/2$ .

According to the tunneling probability, the electronic occupation of orbits, and LED for molecule orbits, the total emission currents for the pristine BNT with different OAs were achieved by integrating the currents from all molecule orbits and all elements of the meshes, which are shown in Fig. 10. The current of the (5, 5) BNT with different OAs is very close to those of CNTs and carbon nanocones [40-41]. The emission currents under lower external fields ( $-0.1$  and  $-0.2 \text{ V/\AA}$ ) are relatively weak, with an order of  $10^{-7} \text{ A}$ . With enhancement in external fields, the potential barrier around the emission spot of the

BNT is lowered, which make it possible to emit the electrons from low-energy molecule orbits. And then deep molecule orbitals would participate in field emission and make larger contribution to total current (with an order of  $10^{-6} \text{ A}$ ). Therefore, the emission currents under  $-0.3\sim-0.5 \text{ V/\AA}$  are evidently larger than that of under  $-0.3\sim-0.2 \text{ V/\AA}$ , with an order of  $10^{-6} \text{ A}$ . Moreover, from Fig. 10, one can find that the total currents increase exponentially with applied fields. However, comparing to the emission currents from all individual states, it is unexpected that possibly the contribution of the same molecule orbit to the

emission current at strong field are less than that at weak field.

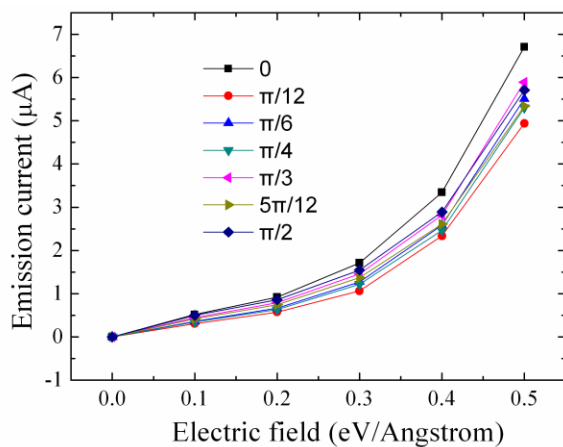


Fig. 10. (Color Online) Emission current versus electric field for the (5, 5) BNTs with different orientation angles.

There is a small distinction among the emission currents under  $-0.1 \text{ V/\AA}$  for the (5, 5) BNT with different orientation angles. However, the distinction was enlarged while the external fields changed from  $-0.1 \text{ V/\AA}$  to higher values. Moreover, the emission currents decrease evidently with orientation angles. The (5, 5) BNT with  $\text{OA}=0$  gains the strongest emission currents under arbitrary electric fields. Therefore, the (5, 5) BNT perpendicular to the substrate is good candidate for field emission devices. Moreover, other types of BNTs (such as (9, 0) and (5, 0) BNTs) are presumed to have similar conclusions as the (5, 5) BNT.

#### 4. Summary

We have researched the influence of orientation angles on electronic and field emission characteristics of the (5, 5) BNT using density functional theory calculations. The calculation results reveal that the boron atoms at the center of emission surface and their adjacent bonds of the BNT are the highest probable positions for electron emission. The emission currents of the (5, 5) BNT under applied electric fields are very close to those of CNTs and carbon nanocones, and their work functions decrease linearly with applied electric fields. The work functions of the BNT decrease/increase regularly with  $E/\text{OA}$ , but the emission currents increase/decrease evidently with  $E/\text{OA}$ . Enhanced/weakened field emission properties by rotating the tube axis are related to change in  $W_f$  and total currents, which are attributed to increase of the  $E_f$  and decrease of the  $V_i$ . The (5, 5) BNT with  $\text{OA}=0$  gained the strongest

emission currents under arbitrary electric fields. Therefore, the (5, 5) BNT with  $\text{OA}=0$  can be strong candidate for electron field emitters.

#### Acknowledgments

We thank the owners of XCrySDen [42-43] and VESTA [44-45]. This letter is benefited from National Natural Science Foundation of China (Grant No. 41476082), a Project of Weifang Science and Technology Program (Grant No. 2014GX041). We also thank Mr. Zhaomin Xu for his perfect advice.

#### References

- [1] S. Iijima, Nature (London) **354**, 56 (1991).
- [2] Q. H. Wang, A. A. Setlur, J. M. Lauerhaas, J. Y. Dai, E. W. Seelig, R. P. H. Chang, Appl. Phys. Lett. **72**, 2912 (1998).
- [3] C. Bower, W. Zhu, D. Shalom, D. Lopez, L. H. Chen, P. L. Gammel, S. Jin, Appl. Phys. Lett. **80**, 3820 (2002).
- [4] H. W. Smith, W. N. J. Lipscomb, Chem. Phys. **43**, 1060 (1965).
- [5] C. E. Nordman, W. N. Lipscomb, J. Chem. Phys. **21**, 1856 (1953).
- [6] W. J. Dulmage, W. N. Lipscomb, Acta Crystallogr. **5**, 260 (1952).
- [7] I. Boustani, A. Quandt, E. Hernandez and A. Rubio, J. Chem. Phys. **110**, 3176 (1999).
- [8] J. Kunstmann, A. Quandt, Phys. Rev. B, **74**, 35413 (2006).
- [9] K. C. Lau, R. Pati, R. Pandey and A. C. Pineda, Chem. Phys. Lett. **418**, 549 (2006).
- [10] H. Tang, S. Ismail-Beigi, Phys. Rev. Lett. **99**, 115501 (2007).
- [11] A. K. Singh, A. Sadrzadeh, B. I. Yakobson, Nano Lett. **8**, 1314 (2008).
- [12] X. Yang, Y. Ding, J. Ni, Phys. Rev. B **77**, 041402 (2008).
- [13] D. Ciuparu, R. F. Klie, Y. Zhu, L. Pfefferle, J. Phys. Chem. B **108**, 3967 (2004).
- [14] F. Liu, C. Shen, Z. Su, X. Ding, S. Deng, J. Chen, N. Xu and H. Gao, J. Mater. Chem. **20**, 2197 (2010).
- [15] J. Liu, Z. Iqbal, MRS Proc. **1307**, 1 (2011).
- [16] I. Boustani and A. Quandt, Europhys. Lett. **39**, 527 (1997).
- [17] S. Suzuki, C. Bower, Y. Watanabe, O. Zhou, Appl. Phys. Lett. **76** 4007 (2000).
- [18] Y. J. Yu, Y. Zhao, S. Ryu, L. E. Brus, K. S. Kim, P. Kim, Nano Lett. **9**, 3430 (2009).

- [19] K. C. Kwon, K. S. Choi, B. J. Kim, J. L. Lee, S. Y. Kim, *J. Phys. Chem. C* **116**, 26586 (2012).
- [20] B. Wang, S. Gunther, J. Wintterlin, M. L. Bocquet, *New J. Phys.* **12**, 043041 (2010).
- [21] Y. Wang, S. W. Tong, X. F. Xu, B. Özyilmaz, K. P. Loh, *Adv. Mater.* **23**, 1514 (2011).
- [22] V. I. Merkulov, A. V. Melechko, M. A. Guillorn, M. L. Simpson, D. H. Lowndes, J. H. Whealton, R. J. Raridon, *Appl. Phys. Lett.* **80**, 4816 (2002).
- [23] C. C. Lin, I. C. Leu, J. H. Yen, M. H. Hon, *Nanotechnology* **15**, 176 (2004).
- [24] A. V. Melechko, V. I. Merkulov, T. E. McKnight, M. A. Guillorn, K. L. Klein, D. H. Lowndes, M. L. Simpson, *J. Appl. Phys.* **97**, 041301 (2005).
- [25] J. F. AuBuchon, L. H. Chen, A. I. Gapin, D. W. Kim, C. Daraio, S. Jin, *Nanoletters* **4**, 1781 (2004).
- [26] G. S. Bocharov, A. V. Eletsii, *Nanomaterials* **3**, 393 (2013).
- [27] V. Bezugly, J. Kunstmann, B. Grundkötter-Stock, T. Frauenheim, T. Niehaus, G. Cuniberti, *ACS Nano* **5**, 4997 (2011).
- [28] J. P. Perdew, K. Burke, M. Ernzerhof, *Phys. Rev. Lett.* **77**, 3865 (1996).
- [29] C. Y. He, Z. Z. Yu, L. Z. Sun, J. X. Zhong, *J. Comput. Theor. Nanosci.* **9**, 16 (2012).
- [30] J. Neugebauer, M. Scheffler, *Phys. Rev. B* **46**, 16067 (1992).
- [31] S. Grimme, *J. Comp. Chem.* **27**, 1787 (2006),
- [32] V. Barone et al., *J. Comp. Chem.* **30**, 934 (2009).
- [33] B. Shan, K. Cho, *Phys. Rev. Lett.* **94**, 236602 (2005).
- [34] See <http://www.quantum-espresso.org/>.
- [35] P. Giannozzi, S. Baroni, N. Bonini, M. Calandra, R. Car, C. Cavazzoni, D. Ceresoli, G. Chiarotti, M. Cococcioni, I. Dabo, A. D. Corso, S. de Gironcoli, S. Fabris, G. Fratesi, R. Gebauer, U. Gerstmann, C. Gougoussis, A. Kokalj, M. Lazzeri, L. Martin-Samos, N. Marzari, F. Mauri, R. Mazzarello, S. Paolini, A. Pasquarello, L. Paulatto, C. Sbraccia, S. Scandolo, G. Sclauzero, A. P. Seitsonen, A. Smogunov, P. Umari, R. M. Wentzcovitch, *J. Phys.: Condens. Mat.* **21**, 395502 (2009).
- [36] M. Khazaei, A. A. Farajian, Y. Kawazoe, *Phys. Rev. Lett.* **95**, 177602 (2005).
- [37] S. F. Xu, G. Yuan, C. Li, W. H. Liu, H. Mimura, *J. Phys. Chem. C* **115**, 8928 (2011).
- [38] Y. Saito, K. Hata, T. Murata, *Jpn. J. Appl. Phys.* **39**, L271 (2000).
- [39] T. Kuzumaki et al., *Diam. Relat. Mater.* **13**, 1907 (2004).
- [40] C. Q. Qu, L. Qiao, C. Wang, S. S. Yu, W. T. Zheng, Q. Jiang, *IEEE Trans. on Nanotech.* **8**, 153 (2009).
- [41] C. Q. Qu, L. Qiao, C. Wang, S. S. Yu, Q. Jiang, W. T. Zheng, *Phys. Lett. A*, **374**, 782 (2010).
- [42] See <http://www.xcrysden.org/>.
- [43] A. Kokalj, *Comput. Mater. Sci.* **28**, 155 (2003).
- [44] See <http://jp-minerals.org/vesta/en/>.
- [45] K. Momma, F. J. Izumi, *Appl. Crystallogr.* **41**, 653 (2008).

---

\*Corresponding author: xushunfu2009@gmail.com